Mon. Not. R. Astron. Soc. **334,** 760–768 (2002)

The impact of an extra background of relativistic particles on the cosmological parameters derived from the cosmic microwave background

R. Bowen,[1]★ S. H. Hansen,[1] A. Melchiorri,[1] Joseph Silk[1] and R. Trotta[2]

[1]*Nuclear and Astrophysics Laboratory, University of Oxford, Keble Road, Oxford OX 3RH*

[2]*Département de Physique Théorique, Université de Genève, 24 quai Ernest Ansermet, CH-1211 Genève 4, Switzerland*

Accepted 2002 April 10. Received 2002 March 1; in original form 2001 November 7

ABSTRACT

Recent estimates of cosmological parameters derived from cosmic microwave background (CMB) anisotropies are based on the assumption that we know the precise amount of energy density in relativistic particles in the Universe, $\omega_{\rm rel}$, at all times. There are, however, many possible mechanisms that can undermine this assumption. In this paper we investigate the effect that removing this assumption has on the determination of the various cosmological parameters. We obtain fairly general bounds on the redshift of equality, $z_{\rm eq} = \omega_m/\omega_{\rm rel} = 3100^{+600}_{-400}$. We show that $\omega_{\rm rel}$ is nearly degenerate with the amount of energy in matter, $\omega_{\rm m}$, and that its inclusion in CMB parameter estimation also affects the present constraints on other parameters such as the curvature or the scalar spectral index of primordial fluctuations. This degeneracy has the effect of limiting the precision of parameter estimation from the *MAP* satellite, but it can be broken by measurements on smaller scales such as those provided by the *Planck* satellite mission.

Key words: cosmic microwave background – cosmological parameters.

1 INTRODUCTION

Our knowledge of the cosmological parameters has increased dramatically with the release of recent cosmic microwave background (CMB) observations (Netterfield et al. 2001; Lee et al. 2001; Halverson et al. 2002). Recent analyses of these data sets (de Bernardis et al. 2001; Wang, Tegmark & Zaldarriaga 2002; Pryke et al. 2002) have reported strong new constraints on various parameters, including the curvature of the universe and the amount of baryonic and dark matter. The precise determination from the CMB of other parameters such as the cosmological constant or the spectral index of primordial fluctuations can be limited by various degeneracies, and such degeneracies are best lifted by combining CMB data with either supernova (SN) data (Garnavich et al. 1998; Perlmutter et al. 1997) or large-scale structure (LSS) surveys, such as PSCz (Saunders et al. 2000), 2dF (Percival et al. 2001) or Lyman α (Croft et al. 2001) data. At present, the values obtained from CMB measurements under the assumption of purely adiabatic fluctuations are consistent with the generic predictions of the inflationary scenario, $n_{\rm s} \sim 1$ and $\Omega_{\rm tot} = 1$ (Linde 1990), and with the standard Big Bang nucleosynthesis bound, $\Omega_{\rm b}h^2 = 0.020 \pm 0.002$ (Burles et al. 2001; Esposito et al. 2001). All of these observations converge towards a consistent picture of our universe, providing strong support for the inflationary scenario as the mechanism which generated the initial conditions for structure formation.

The derivation of the cosmological parameters from CMB is, however, an *indirect* measurement, relying on the assumptions of a theoretical scenario. For this reason, recent efforts have been made to study the effects of the removal of some of these assumptions. For example, a scale-invariant background of gravity waves, generally expected to be small, has been included in the analysis of Kinney, Melchiorri & Riotto (2001); Wang et al. (2002) and Efstathiou et al. (2002), with important consequences for parameter estimation. A scale-dependence of the spectral index has been included in the analysis of Griffiths, Silk & Zaroubi (2001), Barriga et al. (2001) and Hannestad et al. (2002). Furthermore, in Bucher, Moodley & Turok (2001), Trotta, Riazuelo & Durrer (2001) and Amendola et al. (2002), the effects of including isocurvature modes, which naturally arise in the most general inflationary scenarios, have been studied, with the finding that the inclusion of these modes can significantly alter the CMB result. Even more drastic alterations have been proposed in Bouchet et al. (2001) and Durrer, Kunz & Melchiorri (2001).

All the above modifications primarily affect the constraints on the curvature and the physical baryon density parameter, $\omega_{\rm b} \equiv \Omega_{\rm b}h^2$, and the scalar spectral index $n_{\rm s}$. Here $\Omega_{\rm b}$ is the density parameter of baryons and $H_0 \equiv 100h$ km s^{-1} Mpc^{-1} is the present Hubble parameter.

In this paper we study another possible modification to the standard scenario, namely variations in the parameter $\omega_{\rm rel} = \Omega_{\rm rel}h^2$ which describes the energy density of relativistic particles at times near decoupling, $T \sim 0.1$ eV. The energy density of relativistic particles can also conveniently be parametrized via the effective number

★E-mail: reb@astro.ox.ac.uk

of relativistic species, $N_{\rm eff}$, see equation (1) below. CMB data analysis with variations in this parameter has been recently undertaken by many authors (Hannestad 2000; Esposito et al. 2001; Orito et al. 2001; Kneller et al. 2001; Hannestad et al. 2002; Hansen et al. 2002; Zentner & Walker 2002), giving rather crude upper bounds that are significantly improved only by including priors on the age of the universe or by including SN or LSS data. It is worth emphasizing that there is little difference in the bounds obtained on the effective number of relativistic species, $N_{\rm eff}$, between old and new CMB data because of the degeneracy, which we will describe in detail below. We focus here on the effects that the inclusion of this parameter, $\omega_{\rm rel}$, has on the constraints of the remaining parameters in the context of purely adiabatic models.

As we will show below (and as observed previously, see e.g. Hu et al. 1999) there is a strong degeneracy between $\omega_{\rm rel}$ and the physical density of non-relativistic matter, $\omega_{\rm m} \equiv \Omega_{\rm m} h^2$. This is important, because an accurate determination of $\omega_{\rm m}$ from CMB observations [and of $\Omega_{\rm m}$, by including the *Hubble Space Telescope* (*HST*) result $h = 0.72 \pm 0.08$] can be useful for a large number of reasons. First of all, determining the cold dark matter (CDM) content, $\omega_{\rm cdm} = \omega_{\rm m} - \omega_{\rm b}$ can shed new light on the nature of dark matter. The thermally averaged product of cross-section and thermal velocity of the dark matter candidate is related to $\omega_{\rm m}$, and this relation can be used to analyse the implications for the mass spectra in versions of the Supersymmetric Standard Model (see e.g. Barger & Kao 2001; Djouadi, Drees & Kneur 2001; Ellis, Nanopoulos & Olive 2001). The value of $\Omega_{\rm m}$ can be determined in an independent way from the mass-to-light ratios of clusters (Turner 2001), and the present value is $0.1 < \Omega_{\rm m} < 0.2$ (Carlberg et al. 1997; Bahcall et al. 2000). Furthermore, a precise measurement of $\Omega_{\rm m}$ will be a key input for determining the redshift evolution of the equation of state parameter $w(z)$ and thus discriminating between different quintessential scenarios (see e.g. Weller & Albrecht 2002).

This paper is structured as follows. In the next section, we briefly review various physical mechanisms that can lead to a change in $\omega_{\rm rel}$ with respect to the standard value. In Section 3, we illustrate how the CMB angular power spectrum depends on this parameter and identify possible degeneracies with other parameters. In Section 4, we present a likelihood analysis from the most recent CMB data and show which of the present constraints on the various parameters are affected by variations in $\omega_{\rm rel}$. Section 5 forecasts the precision in the estimation of cosmological parameters for the future space missions *MAP* and *Planck*.[1] Finally, in Section 6, we discuss our results and present our conclusions.

2 EFFECTIVE NUMBER OF RELATIVISTIC SPECIES

In the standard model $\omega_{\rm rel}$ includes photons and neutrinos, and it can be expressed as

$$\omega_{\rm rel} = \omega_\gamma + (N_{\rm eff}\omega_\nu) \tag{1}$$

where ω_γ is the energy density in photons and ω_ν is the energy density in one active neutrino. In geometrical units, where $G = \hbar = c = 1$, one has $\omega_x = (4\pi^3/45) g_x T_x^4$, where g_x and T_x are the relativistic degrees of freedom and the temperature of species $x = \gamma, \nu$, respectively. Measuring $\omega_{\rm rel}$ thus gives a direct observation on the effective number of neutrinos, $N_{\rm eff}$. Naturally there are only three active neutrinos, and $N_{\rm eff}$ is simply a convenient parametrization for the extra possible relativistic degrees of freedom

$$N_{\rm eff} = 3 + \Delta N_{\rm CMB}. \tag{2}$$

Thus $\omega_{\rm rel}$ includes energy density from all the relativistic particles: photons, neutrinos, and additional hypothetical relativistic particles such as a light majoron or a sterile neutrino. Such hypothetical relativistic particles are strongly constrained from standard Big Bang nucleosynthesis (BBN), where the allowed extra relativistic degrees of freedom typically are expressed through the effective number of neutrinos, $N_{\rm eff} = 3 + \Delta N_{\rm BBN}$. BBN bounds are typically about $\Delta N_{\rm BBN} < 0.2$–1.0 (Burles et al. 1999; Lisi, Sarkar & Villante 1999).

One should, however, be careful when comparing the effective number of neutrino degrees of freedom at the time of BBN (neutrino decoupling) and at the formation of the cosmic microwave background radiation (CMBR) (photon decoupling) (Hansen et al. 2002). This is because the energy density in relativistic species may change from the time of BBN ($T \sim$ MeV) to the time of last rescattering ($T \sim$ eV). For instance, if one of the active neutrinos has a mass in the range eV $< m <$ MeV and decays into sterile particles such as other neutrinos, majorons, etc., with lifetime t(BBN) $< \tau < t$(CMBR), then the effective number of neutrinos at CMBR would be substantially different from the number at BBN (White, Gelmini & Silk 1995). Such massive active neutrinos, however, do not look too natural any longer, in view of the recent experimental results on neutrino oscillations (Fogli et al. 2002; Gonzalez-Garcia et al. 2001) which show that all active neutrinos are likely to have masses smaller than an eV. One could instead consider sterile neutrinos mixed with active ones that could be produced in the early universe by scattering, and then subsequently decay. The mixing angle must then be large enough to thermalize the sterile neutrinos (Langacker 1989), and this can be expressed through the sterile-to-active neutrino number density ratio $n_s/n_\nu \approx 4 \times 10^4 \sin^2 2\theta \, (m/\text{keV}) \, (10.75/g^*)^{3/2}$ (Dolgov & Hansen 2002), where θ is the mixing angle, and g^* counts the relativistic degrees of freedom, such that $n_s/n_\nu = 1$ or $\Delta g^* = 7/8$ increases $N_{\rm eff}$ by one unit. With n_s/n_ν of order unity, we use the decay time $\tau \approx 10^{20} \, (\text{keV}/m)^5/\sin^2 2\theta$ s and find $\tau \approx 10^{17} \, (\text{keV}/m)^4$ yr, which is much longer than the age of the universe for $m \sim$ keV, so they would certainly not have decayed at t(CMBR). A sterile neutrino with mass of a few MeV would seem to have the right decay time, $\tau \sim 10^5$ yr, but this is excluded by standard BBN considerations (Kolb et al. 1991; Dolgov, Hansen & Semikoz 1998). More inventive models with particles decaying during last rescattering cannot simply be treated with an $N_{\rm CMB}$ that is constant in time, (see e.g. Kaplinghat et al. 1999), and we will not discuss such possibilities further here.

Even though the simplest models predict that the relativistic degrees of freedom are the same at BBN and CMB times, one could imagine more inventive models, such as quintessence (Albrect & Skordis 2000; Skordis & Albrect 2002), which effectively could change ΔN between BBN and CMB (Bean, Hansen & Melchiorri 2001). Naturally, ΔN can be both positive and negative. For BBN, ΔN can be negative if the electron neutrinos have a non-zero chemical potential (Kang & Steigman 1992; Kneller et al. 2001), or more generally with a non-equilibrium electron neutrino distribution function (see e.g. Hansen & Villante 2000). To give an explicit (but highly exotic) example of a different number of relativistic degrees of freedom between BBN and CMB, one could consider the following scenario. Imagine another two sterile neutrinos, one of which is essentially massless and has a mixing angle with any of the active neutrinos just big enough to bring it into equilibrium in the early universe, and one with a mass of $m_{\nu_s} = 3$ MeV and decay

[1] See http://map.gsfc.nasa.gov/ for the *MAP* web site and http://astro.estec.esa.nl/Planck for the *Planck* web site.

time $\tau_{\nu_s} = 0.1$ s, in the decay channel $\nu_s \to \nu_e + \phi$, with ϕ a light scalar. The resulting non-equilibrium electron neutrinos happen to cancel the effect of the massless sterile state exactly, and hence we have $\Delta N_{\rm BBN} = 0$. However, for CMB the picture is much simpler, and we have just the stable sterile state and the majoron, hence $\Delta N_{\rm CMB} = 1.57$. For CMB, one can imagine a negative ΔN from decaying particles, where the decay products are photons or electron/positrons, which essentially increases the photon temperature relative to the neutrino temperature (Kaplinghat & Turner 2001). Such a scenario naturally also dilutes the baryon density, and the agreement on $\omega_{\rm b}$ from BBN and CMB gives a bound on how negative $\Delta N_{\rm CMB}$ can be. Considering all these possibilities, we will therefore not make the usual assumption, $\Delta N_{\rm BBN} = \Delta N_{\rm CMB}$, but instead consider $\Delta N_{\rm CMB}$ as a completely free parameter in the following analysis.

The standard model value for $N_{\rm eff}$ with three active neutrinos is 3.044. This small correction arises from the combination of two effects arising around the temperature $T \sim$ MeV. These effects are the finite temperature QED correction to the energy density of the electromagnetic plasma (Heckler 1994), which gives $\Delta N = 0.01$ (Lopez & Turner 1999; Lopez et al. 1999). If there are more relativistic species than active neutrinos, then this effect will be correspondingly higher (Steigman 2001). The other effect comes from neutrinos sharing in the energy density of the annihilating electrons (Dicus et al. 1982), which gives $\Delta N = 0.034$ (Dolgov, Hansen & Semikoz 1997,1999; Esposito et al. 2000). Thus one finds $N_{\rm eff} = 3.044$. It still remains to accurately calculate these two effects simultaneously. [2]

3 CMB THEORY AND DEGENERACIES

The structure of the C_ℓ spectrum essentially depends on four cosmological parameters:

$$\omega_{\rm b}, \omega_{\rm m}, \omega_{\rm rel} \quad \text{and} \quad \mathcal{R}, \tag{3}$$

defined as: the physical baryonic density $\omega_{\rm b} \equiv \Omega_{\rm b} h^2$, the energy density in matter $\omega_{\rm m} \equiv (\Omega_{\rm cdm} + \Omega_{\rm b})h^2$, the energy density in radiation $\omega_{\rm rel}$ and the 'shift' parameter $\mathcal{R} \equiv \ell_{\rm ref}/\ell$, which gives the position of the acoustic peaks with respect to a flat, $\Omega_\Lambda = 0$ reference model. Here h denotes the Hubble parameter today, $H_0 \equiv 100h$ km s^{-1} Mpc^{-1}, and Ω_Λ is the density parameter due to a cosmological constant, $\Omega_\Lambda \equiv \Lambda/3H_0^2$. In previous analyses (Efstathiou & Bond 1999; Melchiorri & Griffiths 2001 and references therein) the parameter $\omega_{\rm rel}$ has been kept fixed to the standard value, while here we will allow it to vary. It is therefore convenient to write $\omega_{\rm rel} = 4.13 \times 10^{-5}(1 + 0.135\Delta N)$ (taking $T_{\rm CMB} = 2.726$ K), where ΔN is the excess number of relativistic species with respect to the standard model, $N_{\rm eff} = 3 + \Delta N$, and we drop the subscript CMB from now on. The shift parameter $\mathcal{R}$ depends on $\Omega_{\rm m} \equiv \Omega_{\rm cdm} + \Omega_{\rm b}$, on the curvature $\Omega_\kappa \equiv 1 - \Omega_\Lambda - \Omega_{\rm m} - \Omega_{\rm rel}$ and on $\Omega_{\rm rel} = \omega_{\rm rel}/h^2$, through

$$\mathcal{R} = 2\left(1 - \frac{1}{\sqrt{1+z_{\rm dec}}}\right) \times \frac{\sqrt{|\Omega_\kappa|}}{\Omega_{\rm m}} \frac{1}{\chi(y)} \left[\sqrt{\Omega_{\rm rel} + \frac{\Omega_{\rm m}}{1+z_{\rm dec}}} - \sqrt{\Omega_{\rm rel}}\right], \tag{4}$$

[2]Subsequently, such an analysis has been performed (Mangano et al. 2002); the result indicates that the combined effect is slightly smaller, $N_{\rm eff} = 3.0395$.

where $z_{\rm dec}$ is a weak function of the physical baryon density (Hu & Sugiyama 1995), and

$$y = \sqrt{|\Omega_\kappa|} \times \int_0^{z_{\rm dec}} {\rm d}z \left[\Omega_{\rm rel}(1+z)^4 + \Omega_{\rm m}(1+z)^3 + \Omega_\kappa(1+z)^2 + \Omega_\Lambda\right]^{-1/2}. \tag{5}$$

The function $\chi(y)$ depends on the curvature of the universe and is y, $\sin(y)$ or $\sinh(y)$ for flat, closed or open models, respectively. Equation (4) generalizes the expression for $\mathcal{R}$ given in Melchiorri & Griffiths (2001) to the case of non-constant $\Omega_{\rm rel}$.

By fixing the four parameters given in (3), or equivalently the set $\omega_{\rm b}$, the redshift of equality $z_{\rm eq} \equiv \omega_{\rm m}/\omega_{\rm rel}$, ΔN and $\mathcal{R}$, one obtains a perfect degeneracy for the CMB anisotropy power spectra on degree and sub-degree angular scales. On larger angular scales, the degeneracy is broken by the late Integrated Sachs–Wolfe (ISW) effect because of the different curvature and cosmological constant content of the models. From the practical point of view, however, it is still very difficult to break the degeneracy, as measurements are limited by 'cosmic variance' on those scales, and because of the possible contribution of gravitational waves.

Allowing ΔN to vary, but keeping the other three parameters ($\omega_{\rm b}$, $z_{\rm eq}$ and $\mathcal{R}$) constant, we obtain nearly degenerate power spectra which we plot in Fig. 1, normalized to the first acoustic peak. The

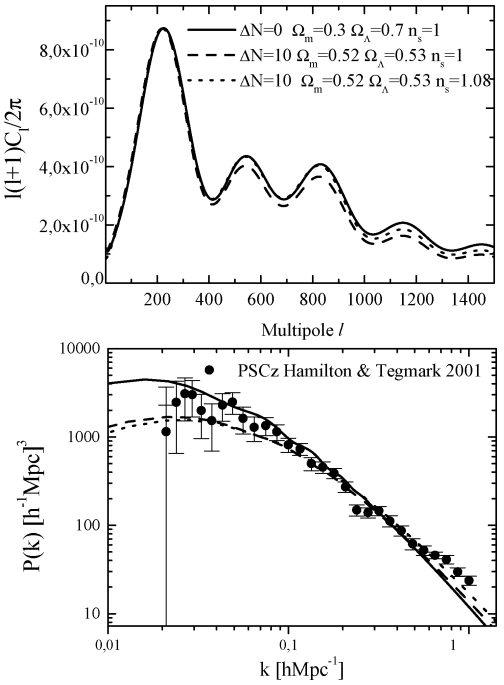

Figure 1. Top panel: CMB degeneracies between cosmological models. Keeping $z_{\rm eq}, \omega_{\rm b}$ and $\mathcal{R}$ fixed while varying ΔN produces nearly degenerate power spectra. The reference model (solid line) has $\Delta N = 0$, $\Omega_{\rm tot} = 1.00$, $n_{\rm s} = 1.00$; the nearly degenerate model (dotted) has $\Delta N = 10$, $\Omega_{\rm tot} = 1.05$, $n_{\rm s} = 1.00$. The curves are normalized to the first peak. The position of the peaks is perfectly matched, only the relative height between the first and the other acoustic peaks is somewhat different in this extreme example, due to the early ISW effect. The degeneracy can be further improved, at least up to the third peak, by raising the spectral index to $n_{\rm s} = 1.08$ (dashed). Bottom panel: the matter power spectra of the models plotted in the top panel together with the observed decorrelated power spectrum from the PSCz survey (Hamilton & Tegmark 2000). The geometrical degeneracy is now lifted.

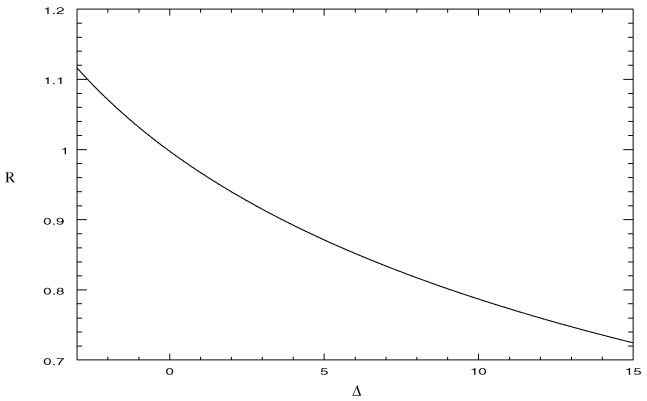

Figure 2. $\mathcal{R}$ as a function of ΔN with $\Omega_\Lambda = 0.7$ and $\Omega_{\rm m} = 0.3$. The position of the peaks is only weakly affected by ΔN.

degeneracy in the acoustic peaks region is now slightly spoiled by the variation of the ratio $\Omega_\gamma / \Omega_{\rm rel}$: the different radiation content at decoupling induces a larger (for $\Delta N > 0$) early ISW effect, which boosts the height of the first peak with respect to the other acoustic peaks. Nevertheless, it is still impossible to distinguish between the different models with present CMB measurements and without external priors. Furthermore, a slight change in the scalar spectral index, $n_{\rm s}$, can reproduce a perfect degeneracy up to the third peak.

The main result of this is that, even with a measurement of the first three peaks in the angular spectrum, it is impossible to put bounds on $\omega_{\rm rel}$ alone, even when fixing other parameters such as $\omega_{\rm b}$. Furthermore, as the degeneracy is mainly in $z_{\rm eq}$, the constraints on $\omega_{\rm m}$ from CMB are also affected (see Section 4).

In Fig. 2 we plot the shift parameter $\mathcal{R}$ as a function of ΔN, while fixing $\Omega_{\rm m} = 0.3$ and $\Omega_\Lambda = 0.7$. Increasing ΔN moves the peaks to smaller angular scales, even though the dependence of the shift parameter on ΔN is rather mild. In order to compensate this effect, one has to change the curvature by increasing $\Omega_{\rm m}$ and Ω_Λ. We therefore conclude that the present bounds on the curvature of the universe are weakly affected by ΔN. Nevertheless, when a positive (negative) ΔN is included in the analysis, the preferred models are shifted toward closed (open) universes.

4 CMB ANALYSIS

In this section we compare the recent CMB observations with a set of models with cosmological parameters sampled as follows: $0.1 < \Omega_m < 1.0$, $0.1 < \Omega_{\rm rel}/\Omega_{\rm rel}(\Delta N = 0) < 3$, $0.015 < \Omega_b < 0.2$; $0 < \Omega_\Lambda < 1.0$ and $0.40 < h < 0.95$. We vary the spectral index of the primordial density perturbations within the range $n_{\rm s} = 0.50, \ldots, 1.50$ and we re-scale the fluctuation amplitude by a pre-factor C_{10}, in units of $C_{10}^{\rm COBE}$. We also restrict our analysis to purely adiabatic, *flat* models ($\Omega_{\rm tot} = 1$) and we add an external Gaussian prior on the Hubble parameter $h = 0.65 \pm 0.2$.

The theoretical models are computed using the publicly available CMBFAST program (Seljak & Zaldarriaga 1996a,b) and are compared with the recent BOOMERanG-98, DASI and MAXIMA-1 results. The power spectra from these experiments were estimated in 19, 9 and 13 bins, respectively, spanning the range $25 \leqslant \ell \leqslant 1100$. We approximate the experimental signal $C_B^{\rm ex}$ inside the bin to be a Gaussian variable, and we compute the corresponding theoretical value $C_B^{\rm th}$ by convolving the spectra computed by CMBFAST with the respective window functions. When the window functions are not available, as in the case of BOOMERanG-98, we use top-hat window functions. The likelihood for a given cosmological model is then defined by $-2\ln L = (C_B^{\rm th} - C_B^{\rm ex}) M_{BB'} (C_{B'}^{\rm th} - C_{B'}^{\rm ex})$, where $C_B^{\rm th}$ ($C_B^{\rm ex}$) is the theoretical (experimental) band power and $M_{BB'}$ is the Gaussian curvature of the likelihood matrix at the peak. We consider 10, 4 and 4 per cent Gaussian distributed calibration errors (in μK) for the BOOMERanG-98, DASI and MAXIMA-1 experiments, respectively. We also include the *COBE* data using Lloyd Knox's RADPack packages (see Bond, Jaffe & Knox 2000).

In order to show the effect of the inclusion of $\omega_{\rm rel}$ on the estimation of the other parameters, we plot likelihood contours in the $\omega_{\rm rel}$–ω_m, $\omega_{\rm rel}$–$\omega_{\rm b}$ and $\omega_{\rm rel}$–$n_{\rm s}$ planes.

Proceeding as in Melchiorri et al. (2000), we calculate a likelihood contour in those planes by finding the remaining 'nuisance' parameters that maximize it. For a Gaussian, maximization is equivalent to marginalization. We then define our 68, 95 and 99 per cent confidence levels to be where the likelihood falls to 0.32, 0.05 and 0.01 of its peak value, as would be the case for a 2D Gaussian.

In Fig. 3, we plot the likelihood contours for $\omega_{\rm rel}$ versus $\omega_{\rm m}$, $\omega_{\rm b}$ and $n_{\rm s}$ (top to bottom). As we can see, $\omega_{\rm rel}$ is very weakly constrained to be in the range $1 \leqslant \omega_{\rm rel}/\omega_{\rm rel}(\Delta N = 0) \leqslant 1.9$ at 1σ in all plots. The degeneracy between $\omega_{\rm rel}$ and ω_m is evident in the top panel of Fig. 3. Increasing $\omega_{\rm rel}$ shifts the epoch of equality and this can be compensated only by a corresponding increase in $\omega_{\rm m}$. It is interesting to note that even if we are restricting our analysis to flat models, the degeneracy is still there and the bounds on $\omega_{\rm m}$ are strongly affected. We find $\omega_{\rm m} = 0.2 \pm 0.1$, which is comparable with $\omega_{\rm m} = 0.13 \pm 0.04$ when ΔN is kept to zero. It is important to realize that these bounds on $\omega_{\rm rel}$ appear because of our prior on h and because we consider flat models. When one allows h as a free parameter and any value for $\Omega_{\rm m}$, then the degeneracy is almost complete and there are no bounds on $\omega_{\rm rel}$. In the middle and bottom panel of Fig. 3 we plot the likelihood contours for $\omega_{\rm b}$ and $n_{\rm s}$. As we can see, these parameters are not strongly affected by the inclusion of $\omega_{\rm rel}$. The bound on $\omega_{\rm b}$, in particular, is completely unaffected by $\omega_{\rm rel}$. There is, however, a small correlation between $\omega_{\rm rel}$ and $n_{\rm s}$: the boost of the first peak induced by the ISW effect can be compensated (at least up to the third peak) by a small change in $n_{\rm s}$.

AS the degeneracy is mainly in $z_{\rm eq}$, it is useful to estimate the constraints we can put on this variable. In Fig. 4 we plot the likelihood curve on $z_{\rm eq}$ by using the marginalization/maximization algorithm described above. By integration of this probability distribution function we obtain $z_{\rm eq} = 3100^{+600}_{-400}$ at 68 per cent confidence limit, i.e. a late-time equality, in agreement with a low-density universe.

4.1 External constraints

It is interesting to investigate how well constraints from independent non-CMB data sets can break the above degeneracy between $\omega_{\rm rel}$ and $\omega_{\rm m}$. The supernovae luminosity distance is weakly dependent on $\omega_{\rm rel}$ (see however Zentner & Walker 2002), and the bounds obtained on $\Omega_{\rm m}$ can be used to break the CMB degeneracy. Including the SN-Ia constraints on the $\Omega_{\rm m}$–Ω_Λ plane, $0.8\Omega_{\rm m} - 0.6\Omega_\Lambda = -0.2 \pm 0.1$ (Perlmutter et al. 1999), we find $\omega_{\rm rel}/\omega_{\rm rel}(\Delta N = 0) = 1.12^{0.35}_{-0.42}$ at the 2σ confidence level.

It is also worthwile to include constraints from galaxy clustering and local cluster abundances. The shape of the matter power spectrum in the linear regime for galaxy clustering can be characterized by the shape parameter $\Gamma \sim \Omega_{\rm m} h / \sqrt{(1 + 0.135\Delta N)}\, {\rm e}^{-[\Omega_{\rm b}(1+\sqrt{2h}/\Omega_{\rm m}) - 0.06]}$. From the observed data one has roughly (see e.g. Bond & Jaffe 1998) $0.15 \leqslant \Gamma + (n_{\rm s} - 1)/2 \leqslant 0.3$. This constraint is in agreement with the recent 2dF survey, where they quote $\Omega_{\rm m} h = 0.20 \pm 0.03$ at 1σ (Percival et al. 2001).

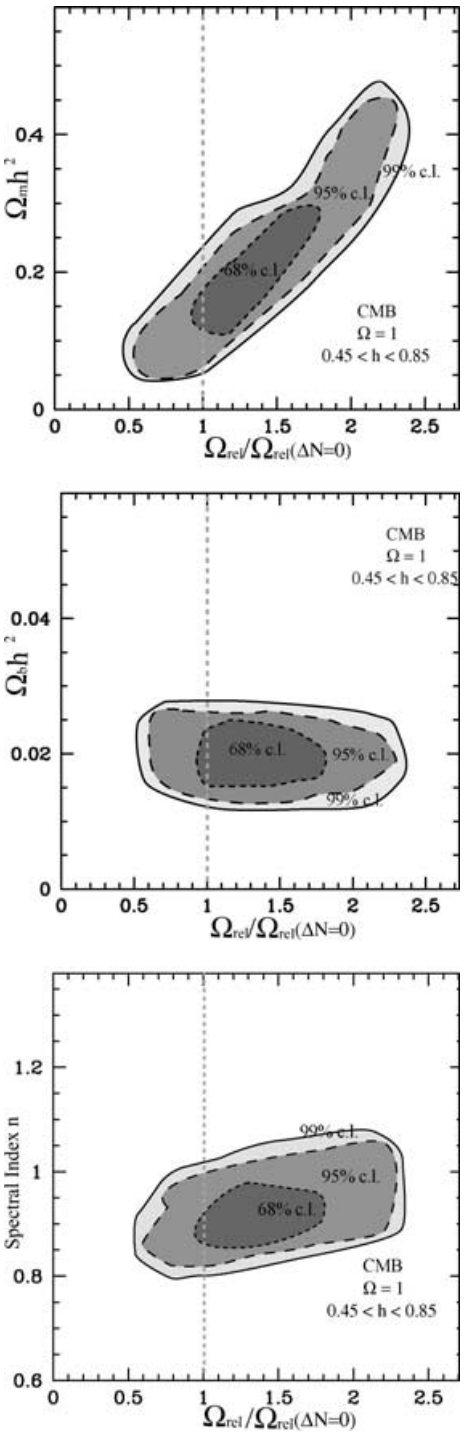

Figure 3. Likelihood curve plots.

The degeneracy between $\omega_{\rm m}$ and $\omega_{\rm rel}$ in the CMB cannot be broken trivially by inclusion of large-scale structure (LSS) data, because a similar degeneracy affects the LSS data as well (see e.g. Hu et al. 1999). However, the geometrical degeneracy is lifted in the matter power spectrum, and accurate measurements of galaxy clustering at very large scales can distinguish between various models. This is exemplified in the bottom panel of Fig. 1, where we plot three matter power spectra with the same cosmological parameters as in the top panel, together with the decorrelated matter power spectrum obtained from the PSCz survey.

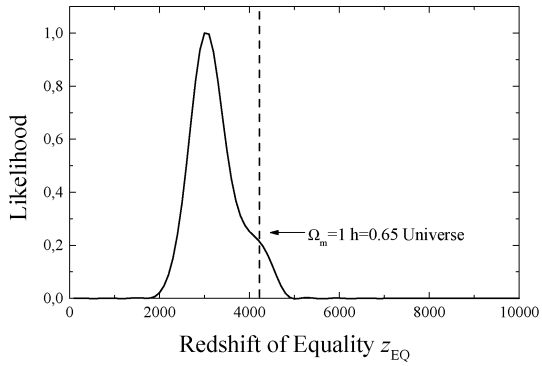

Figure 4. Likelihood probability distribution function for the redshift of equality.

Table 1. Data analysis results: 2σ confidence intervals on the effective energy density of relativistic particles, $\omega_{\rm rel}/\omega_{\rm rel}(\Delta N=0)$, and on the corresponding effective number of neutrino species, $N_{\rm eff}$, for different data set combinations. Note that the bounds obtained with CMB data only mainly reflect the priors used in the anlysis.

	$\omega_{\rm rel}/\omega_{\rm rel}\,(\Delta N=0)$	$N_{\rm eff}$
CMB only	$1.50^{+0.90}_{-0.90}$	0.04, . . . , 13.37
CMB + SN-Ia	$1.12^{+0.35}_{-0.42}$	0.78, . . . , 6.48
CMB + PSCz	$1.40^{+0.49}_{-0.56}$	1.81, . . . , 9.59
CMB + σ_8	$1.27^{+0.35}_{-0.43}$	1.82, . . . , 7.59

The inclusion of the above (conservative) value on Γ assumed with a Gaussian-shaped function, gives $\omega_{\rm rel}/\omega_{\rm rel}\,(\Delta N=0)=1.40^{0.49}_{-0.56}$, which is less restrictive than the one obtained with the SN-Ia prior.

A better constraint can be obtained by including a prior on the variance of matter perturbations over a sphere of size $8h^{-1}$ Mpc, derived from cluster abundance observations. Comparing with $\sigma_8=(0.55\pm 0.05)\Omega_{\rm m}^{-0.47}$ at $1-\sigma$, we obtain $\omega_{\rm rel}/\omega_{\rm rel}\,(\Delta N=0)=1.27^{0.35}_{-0.43}$, again at the 2σ confidence level.

Our results are summarized in Table 1. The combination of present-day CMB data with SN and LSS data yields a lower bound $N_{\rm eff}>0.8$ and >1.8, respectively, at the 2σ confidence level. Our result is in good agreement with the analysis in Hannestad (2001), which considered similar data sets. It is worth emphasizing the fact that $N_{\rm eff}=0$ is excluded at much more than 2σ: this can be considered as a strong cosmological evidence of the presence of a neutrino background, as predicted by the Standard Model. The upper bounds for the combined sets can be expressed as $N_{\rm eff}<6.5$ for CMB + SN and $N_{\rm eff}<9.6$ for CMB + LSS, at 2σ.

5 FORECAST FOR *MAP* AND *PLANCK*

In this section we perform a Fisher matrix analysis in order to estimate the precision with which forthcoming satellite experiments will be able to constrain the parameter $z_{\rm eq}$.

5.1 Fisher matrix

Using $\mathcal{L}(\mathbf{s})$ to denote the likelihood function for the parameter set $\mathbf{s}$ and expanding $\ln\mathcal{L}$ to quadratic order about the maximum defined

by the reference model parameters s_0, one obtains

$$\mathcal{L} \approx \mathcal{L}(s_0) \exp\left(-\frac{1}{2} \sum_{i,j} \mathbf{F}_{ij} \delta s_i \delta s_j \right)$$

where the *Fisher matrix* $\mathbf{F}_{ij}$ is given by the expression

$$\mathbf{F}_{ij} = \sum_{\ell}^{\ell_{\max}} \frac{1}{(\Delta C_\ell)^2} \frac{\partial C_\ell}{\partial s_i} \frac{\partial C_\ell}{\partial s_j} \tag{6}$$

and $\ell_{\max}$ is the maximum multipole number accessible to the experiment. The quantity ΔC_ℓ is the standard deviation on the estimate of C_ℓ, which takes into account both cosmic variance and the expected error of the experimental apparatus and is given by

$$(\Delta C_\ell)^2 \approx \frac{2}{(2\ell+1) f_{\rm sky}} \left(C_\ell + \bar{\mathcal{B}}_\ell^2 \right)^2, \tag{7}$$

$$\bar{\mathcal{B}}_\ell^2 = \sum_c w_c \mathrm{e}^{[-\ell(\ell+1)/\ell_c^2]} \tag{8}$$

(Knox 1995; Efstathiou & Bond 1999), for an experiment with N channels (denoted by a subscript c), angular resolution (full width at half maximum, FWHM) θ_c, sensitivity σ_c per resolution element and with a sky coverage $f_{\rm sky}$. The inverse weight per solid angle is $w_c^{-1} \equiv (\sigma_c \theta_c)^{-2}$ and $\ell_c \equiv \sqrt{8 \ln 2}/\theta_c$ is the width of the beam, assuming a Gaussian profile. If the initial fluctuations are Gaussian and a uniform prior is assumed, one finds that the covariance matrix is given by the inverse of the Fisher matrix, $\mathbf{C} = \mathbf{F}^{-1}$ (Bond, Efstathiou & Tegmark 1997). The standard deviation for the parameter s_i (with marginalization over all other parameters) is therefore given by $\sigma_i = \sqrt{C_{ii}}$. This approximation is rigorously valid only in the vicinity of the maximum of the likelihood function, but it has proved to give useful insight even for large values of $s - s_0$ (Efstathiou & Bond 1999; Efstathiou 2001). The main advantage of the Fisher matrix approach when compared to an exact likelihood analysis is that for m cosmological parameters the former requires only the evaluation of $m + 1$ power spectra. Therefore the computational effort is vanishingly small with respect to the one necessary for a full likelihood analysis of the parameter space.

Table 2 summarizes the experimental parameters for *MAP* and *Planck* we have used in the analysis. For both experiment we have taken $f_{\rm sky} = 0.50$. These values are indicative of the expected performance of the experimental apparatus, but the actual values may be somewhat different, especially for the *Planck* satellite.

5.2 Cosmological parameters

The validity of the Fisher matrix analysis depends on the chosen parameter set, as well as on the point s_0 at which the likelihood function is supposed to reach its maximum. We use the following nine-dimensional parameter set: $\omega_{\rm b}$, ω_c, ω_Λ, $\mathcal{R}$, $z_{\rm eq}$, $n_{\rm s}$, $n_{\rm t}$, r, Q.

Table 2. Experimental parameters used in the Fisher matrix analysis for *MAP* (first three channels) and *Planck* (last four channels).

	MAP			*Planck*			
ν (GHz)	40	60	90	100	150	220	350
θ_c (degrees)	0.46	0.35	0.21	0.18	0.13	0.09	0.08
$\sigma_c/10^{-6}$	6.6	12.1	25.5	1.7	2.0	4.3	14.4
$w_c^{-1}/10^{-15}$	2.9	5.4	6.8	0.028	0.022	0.047	0.44
ℓ_c	289	385	642	757	1012	1472	1619
$\ell_{\max}$		1500			2000		

Here $n_{\rm s}$, $n_{\rm t}$ are the scalar and tensor spectral indices respectively, $r = C_2^T/C_2^S$ is the tensor-to-scalar ratio at the quadrupole, and $Q = \langle \ell(\ell+1) C_\ell \rangle^{1/2}$ denotes the overall normalization, where the mean is taken over the multipole range accessible to the experiment. We choose to use the shift parameter $\mathcal{R}$ because this takes into account the geometrical degeneracy between Ω_Λ and Ω_κ (Efstathiou & Bond 1999). Our purely adiabatic reference model has parameters: $\omega_{\rm b} = 0.0200$ ($\Omega_{\rm b} = 0.0473$), $\omega_c = 0.1067$ ($\Omega_c = 0.2527$), $\omega_\Lambda = 0.2957$ ($\Omega_\Lambda = 0.7000$), ($h = 0.65$), $\mathcal{R} = 0.953$, $z_{\rm eq} = 3045$, $n_{\rm s} = 1.00$, $n_{\rm t} = 0.00$, $r = 0.10$, $Q = 1.00$. This is a fiducial, concordance model, which we believe is in good agreement with most recent determinations of the cosmological parameters (flat universe, scale invariant spectral index, BBN compatible baryon content, large cosmological constant). Furthermore, we allow for a modest, 10 per cent tensor contribution at the quadrupole in order to be able to include tensor modes in the Fisher matrix analysis.

We plot the derivatives of C_ℓ with respect to the different parameters in Fig. 5 . Generally, we remark that derivatives with respect to the combination of parameters describing the matter content of the universe ($\omega_{\rm b}$ and ω_c, $\mathcal{R}$, $z_{\rm eq}$) are large in the acoustic peaks region, $\ell > 100$, while derivatives with respect to parameters describing the tensor contribution ($n_{\rm t}$, r) are important in the large angular scale region. Because measurements in this region are cosmic-variance limited, we expect uncertainties in the latter set of parameters to be large regardless of the details of the experiment. The curve for $\partial C_\ell/\partial Q$ is of course identical to the C_ℓ values themselves. The cosmological constant is a notable exception: variation in the value of ω_Λ keeping all other parameters fixed produces a perfect degeneracy in the acoustic peaks region. Therefore we expect the derivative $\partial C_\ell/\partial \omega_\Lambda$ to be 0 in this region. Small numerical errors in the computation of the spectra, however, artificially spoil this degeneracy, erroneously leading to smaller predicted uncertainties. In order to suppress this effect, we set $\partial C_\ell/\partial \omega_\Lambda = 0$ for $\ell > 200$. From equation (6) we see that a large absolute value of $\partial C_\ell/\partial s_i$ leads to a large F_{ii} and therefore to a smaller 1σ error (roughly neglecting non-diagonal contributions). If the derivative along s_i can be approximated as a linear combination of the others, however, then the corresponding directions in parameter space will be degenerate, and the expected error will be important. This is the case for mild, featureless derivatives as $\partial C_\ell/\partial r$, while wild changing derivatives (such as $\partial C_\ell/\partial \mathcal{R}$) induce smaller errors in the determination of the corresponding parameter. Therefore the choice of the parameter set is very important in order to correctly predict the standard errors of the experiment.

5.3 Error forecast

The quantity $\epsilon_i \equiv 1/\sqrt{\lambda_i}$, where λ_i is the ith eigenvalue of the Fisher matrix, sometimes used as a rough indication of the power of an experiment. It expresses the accuracy with which the ith eigenvector of the Fisher matrix can be determined. For *MAP* (Planck) the number of eigenvectors with $\epsilon_i < 10^{-3}$ is 1/9 (3/9) and with $\epsilon_i < 10^{-2}$ is 3/9 (6/9). It is important to keep in mind, however, that the actual quantities one is interested in are the physical parameters rather than linear combinations of them such as the principal components.

Table 3 shows the results of our analysis for the expected 1σ error on the physical parameters. Determination of the redshift of equality can be achieved by *MAP* with 23 per cent accuracy, while *Planck* will pinpoint it down to 2 per cent or so. From $\omega_{\rm rel} = (\omega_{\rm b} + \omega_c)/z_{\rm eq}$ it follows that the energy density of relativistic particles, $\omega_{\rm rel}$, will be determined within 43 per cent by *MAP* and 3 per cent by *Planck*.

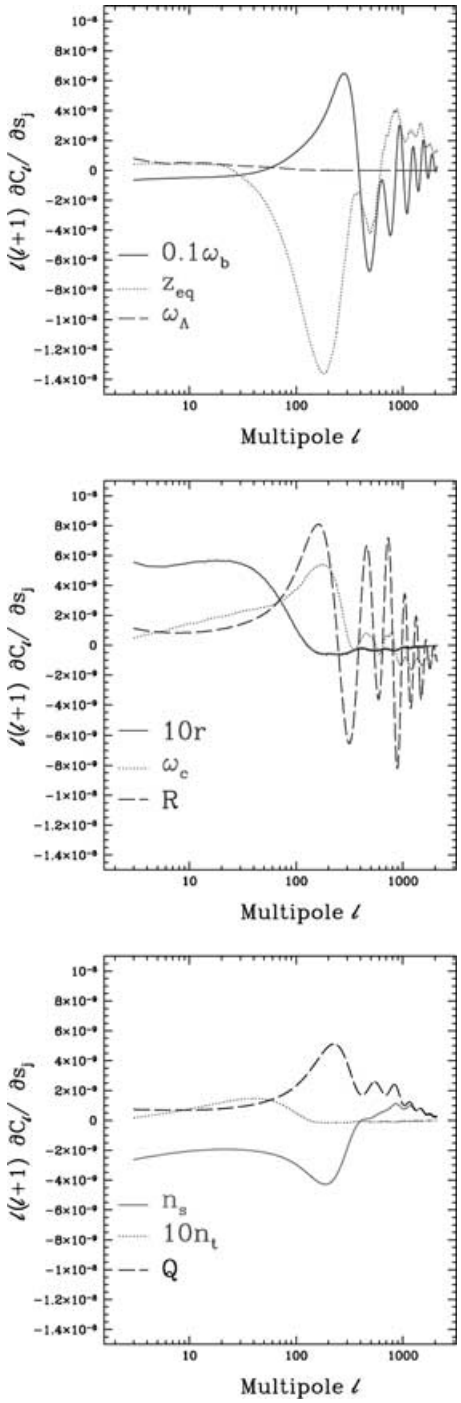

Figure 5. Derivatives of C_ℓ with respect to the nine parameters evaluated at the reference model described in the text. The numerical prefactor indicates that the corresponding curve has been rescaled: thus $0.1\omega_b$ means that the displayed curve is $0.1(\partial C_\ell/\partial\omega_b)$. The derivative $\partial C_\ell/\partial\omega_\Lambda$ has been set to 0 for $\ell > 200$ in order to suppress the effect of numerical errors, thus taking into account the geometrical degeneracy.

This translates into an impossibility for *MAP* of measuring the effective number of relativistic species ($\Delta N_{\rm eff} \approx 3.17$ at 1σ), while *Planck* will be able to track it down to $\Delta N_{\rm eff} \approx 0.24$. As for the other parameters, while the position of the acoustic peaks (through the value of $\mathcal{R}$) and the matter content of the universe can be determined by *Planck* with high accuracy (of the order of or less than 1 per cent), the cosmological constant remains (with CMB data only) almost undetermined, because of the effect of the geometrical degeneracy. The scalar spectral index n_s and the overall normalization will be well constrained already by *MAP* (within 15 per cent and 1 per cent, respectively), while because of the reasons explained above the tensor spectral index n_t and the tensor contribution r will remain largely unconstrained by both experiments. Generally, an improvement of a factor of 10 is to be expected between *MAP* and *Planck* in the determination of most cosmological parameters.

Table 3. Fisher matrix analysis results: expected 1σ errors for the *MAP* and *Planck* satellites. See the text for details and discussion.

	MAP	*Planck*
$\delta z_{\rm eq}/z_{\rm eq}$	0.23	0.02
$\delta\omega_{\rm rel}/\omega_{\rm rel}$	0.43	0.03
$\Delta N_{\rm eff}$	3.17	0.24
$\delta\omega_{\rm b}/\omega_{\rm b}$	0.12	<0.01
$\delta\omega_c/\omega_c$	0.50	0.04
$\delta\omega_\Lambda/\omega_\Lambda$	3.40	1.71
$\delta\mathcal{R}$	<0.01	<0.01
$\delta n_{\rm s}$	0.15	0.01
$\delta n_{\rm t}$	1.96	1.08
$\delta r/r$	5.22	2.67
δQ	0.01	<0.01

Our analysis considers temperature information only. Inclusion of polarization measurements would tighten errors, especially for the 'primordial' parameters n_s, n_t and r (Zaldarriaga, Spergel & Seljak 1997; Bucher et al. 2001). This is especially important for a *MAP*-type experiment, as a precise determination of n_s and an higher accuracy in ω_m would greatly improve the precision on $N_{\rm eff}$ which can be obtained with temperature only. By the time *Planck* will obtain its first results, polarization measurements will hopefully have been performed. Combination of polarization information with the *MAP* temperature data would then considerably improve the precision of the extracted parameter values.

A Fisher matrix analysis for $\Delta N_{\rm eff}$ was previously performed by Lopez et al. (1999) and repeated by Kinney & Riotto (1999) (with the equivalent chemical potential ξ, $\Delta N = 15/7[2(\xi/\pi)^2 + (\xi/\pi)^4]$, and a strong degeneracy was found between $N_{\rm eff}$, h and Ω_Λ, and to lesser extent with Ω_b. We have seen here that the degeneracy really is between $\omega_{\rm rel}$, ω_m and n_s, and the degeneracy previously observed is thus explained because they considered flat models, where a change in Ω_Λ is equivalent to a change in ω_m, $\omega_m = (1 - \Omega_\Lambda - \Omega_b)h^2$. The results of this paper, on how precisely the future satellite missions can extract the relativistic energy density, can be translated into approximately $\Delta N_{\rm eff} = 3.17$ ($\xi = 2.4$) and $\Delta N_{\rm eff} = 0.24$ ($\xi = 0.73$) for *MAP* and *Planck* respectively. However, including neutrino oscillation leads to equilibration of the different chemical potentials, and hence BBN leads to the stronger bound $|\xi| < 0.07$ for all neutrino species (Dolgov et al. 2002).

6 CONCLUSIONS

In this paper, we have examined the effect of varying the background of relativistic particles on the cosmological parameters derived from CMB observations. We have found that the present constraints on the overall curvature, Ω_κ, and tilt of primordial fluctuations, n_s, are slightly affected by the inclusion of this background. However, we

have found a relevant degeneracy with the amount of non-relativistic matter $\omega_{\rm m}$. Even with relatively strong external priors (flatness, $h = 0.65 \pm 0.2$, age > 10 Gyr) the present CMB bound (95 per cent confidence limit) $0.1 < \omega_{\rm m} < 0.2$ spreads to $0.05 < \omega_{\rm m} < 0.45$ when variations in $\omega_{\rm rel}$ are allowed. Specifically, without priors on $\omega_{\rm m}$ (through flatness, h, etc) no bounds on $N_{\rm eff}$ can be obtained. Combination of present-day CMB data with SN (with LSS) data gives $0.8(1.8) < N_{\rm eff} < 6.5(9.6)$, at 2σ confidence level. The lower bound can be considered as a cosmological evidence of the presence of a neutrino background, as predicted by the Standard Model.

Another fundamental point bears on the identification of the best choice of parameters, i.e. parameter combinations which can be unambigously extracted from CMB data. It is of the greatest importance to realize which parameter set is least plagued by degeneracy problems, i.e. which directions in parameter space are non-flat. In the well known case of the geometrical degeneracy, the shift parameter $\mathcal{R}$ can be determined with very high precision by measuring the position of the peaks. The curvature and the Hubble parameters, however, are almost flat directions in parameter space, and therefore are not ideal variables for extraction from CMB data. In this work, we have pointed out that an analogous situation exists for $z_{\rm eq}$, $\omega_{\rm rel}$ and $\omega_{\rm m}$. In fact, $z_{\rm eq}$ is well determined because it measures the physical distance to equality time, while on the contrary $\omega_{\rm m}$ is a rather ill-suited variable for CMB data, as it suffers from degeneracy with $\omega_{\rm rel}$ (at least up to the third acoustic peak).

Fortunately, as we saw in the last section, the matter–radiation degeneracy in the CMB data is present only up to the third peak and future space missions like *Planck* will be able to determine separately the amount of matter and radiation in the universe.

ACKNOWLEDGMENTS

It is a pleasure to thank the referee Andrew Jaffe for useful comments. We thank C. Boehm, R. Durrer, L. M. Griffiths, M. Kaplinghat and A. Riazuelo for useful discussions. TR is grateful to the University of Oxford for the hospitality during part of this work. SHH is supported by a Marie Curie Fellowship of the European Community under the contract HPMFCT-2000-00607. AM is supported by PPARC. This work is supported by the European Network CMBNET.

REFERENCES

Albrect A., Skordis C., 2000, Phys. Rev. Lett., 84, 2076
Amendola L., Gordon C., Wands D., Sasaki M., 2002, Phys. Rev. Lett., 88, 211302
Bahcall N., Cen. R., Davé R., Ostriker J. P., Yu Q., 2000, ApJ, 541, 1
Barger V., Kao C., 2001, Phys. Lett. B, 518, 117
Barriga J., Gaztañaga E., Santos M. G., Sarkar S., 2001, MNRAS, 324, 977
Bean R., Hansen S. H., Melchiorri A., 2001, Phys. Rev. D, 64, 103508
de Bernardis P. et al., 2000, Nat, 404, 955
Bond J. R., Jaffe A. H., 1998, Phil. Soc. Trans. R. Soc. London, Meeting on Large Scale Structure in the universe. Royal Society, London
Bond R. J., Efstathiou G., Tegmark M., 1997, preprint (astro-ph/9702100)
Bond J. R., Jaffe A. H., Knox L. E., 2000, ApJ, 533, 19
Bouchet F. R., Peter P., Riazuelo A., Sakellariadou M., 2002, Phys. Rev. D, 65, 021301
Bucher M., Moodley K., Turok T., 2001, Phys. Rev, Lett., 87, 191301
Burles S., Nollett K. M., Truran J. N., Turner M. S., 1999, Phys. Rev. Lett., 82, 4176
Carlberg R. G., Morris S. L., Yee H. K. C., Ellingson E., 1997, ApJL, in press (astro-ph/9612169)
Croft R. A. C., Weinberg D. H., Bolte M., Burles S., Hernquist L., Katz N., Kirkman D., Tytler D., 2000, ApJ, submitted (astro-ph/0012324)
Dicus D. A., Kolb E. W., Gleeson A. M., Sudarshan E. C., Teplitz V. L., Turner M. S., 1982, Phys. Rev. D, 26, 2694
Djouadi A., Drees M., Kneur J. L., 2001, JHEP, 0108, 055
Dolgov A. D., Hansen S. H., 2002, Astropart. Phys., 16, 339
Dolgov A. D., Hansen S. H., Semikoz D. V., 1997, Nucl. Phys. B, 503, 426
Dolgov A. D., Hansen S. H., Semikoz D. V., 1998, Nucl. Phys. B, 524, 621
Dolgov A. D., Hansen S. H., Semikoz D. V., 1999, Nucl. Phys. B, 543, 269
Dolgov A. D., Hansen S. H., Pastor S., Petcov S. T., Raffelt G. G., Semikoz D. V., 2002, Nucl. Phys. B, 632, 363
Durrer R., Kunz M., Melchiorri A., 2001, Phys. Rev. D, 63, 081301
Efstathiou G., 2001, MNRAS, 332, 193
Efstathiou G., Bond J. R., 1999, MNRAS, 304, 75
Efstathiou G. et al. (2dFGRS Team), 2002, MNRAS, 330, L29
Eisenstein D. J., Hu W., Tegmark M., 1998, ApJL, submitted (astro-ph/9805239)
Ellis J. R., Nanopoulos D. V., Olive K. A., 2001, Phys. Lett. B, 508, 65
Esposito S., Miele G., Pastor S., Peloso M., Pisanti O., 2000, Nucl. Phys. B, 590, 539
Esposito S., Mangano G., Melchiorri A., Miele G., Pisanti O., 2001, Phys. Rev. D, 63, 043004
Fogli G. L., Lisi E., Marrone A., Montanino D., Palazzo A., 2002, Phys. Rev. D, 65, 073008
Garnavich P. M. et al., 1998, ApJ, 493, L53
Gonzalez-Garcia M. C., Maltoni M., Pena-Garay C., Valle J. W. F., 2001, Phys. Rev. D, 63, 033005
Griffiths L. M., Silk J., Zaroubi S., 2001, MNRAS, 324, 712
Halverson N. W. et al., 2002, ApJ, 568, 384
Hannestad S., 2000, Phys. Rev. Lett., 85, 4203
Hannestad S., 2001, Phys. Rev. D, 64, 083002
Hannestad S., Hansen S. H., Villante F. L., Hamilton A. J., 2002, Astropart. Phys., 17, 375
Hansen S. H., Villante F. L., 2000, Phys. Lett. B, 486, 1
Hansen S. H., Mangano G., Melchiorri A., Miele G., Pisanti O., 2002, Phys. Rev. D, 65, 023511
Heckler A. F., 1994, Phys. Rev. D, 49, 611
Hu W., Sugiyama N., 1995, Phys. Rev. D, 51, 2599
Hu W., Eisenstein D. J., Tegmark M., White M. J., 1999, Phys. Rev. D, 59, 023512
Kang H., Steigman G., 1992, Nucl. Phys. B, 372, 494
Kaplinghat M., Turner M. S., 2001, Phys. Rev. Lett., 86, 385
Kaplinghat M., Lopez R. E., Dodelson S., Scherrer R. J., 1999, Phys. Rev. D, 60, 123508
Kinney W. H., Riotto A., 1999, Phys. Rev. Lett., 83, 3366
Kinney W., Melchiorri A., Riotto A., 2001, Phys. Rev. D, 63, 023505
Kneller J. P., Scherrer R. J., Steigman G., Walker T. P., 2001, Phys. Rev. D, 64, 123506
Knox L., 1995, Phys. Rev. D, 52, 4307
Kolb E. W., Turner M. S., Chakravorty A., Schramm D. N., 1991, Phys. Rev. Lett., 67, 533
Langacker P., 1989, UPR-0401T
Lee A. T. et al., 2001, ApJ, 561, L1
Linde A. D., 1990, Particle Physics And Inflationary Cosmology. Harwood Academic, Chur, Switzerland, p. 5
Lisi E., Sarkar S., Villante F. L., 1999, Phys. Rev. D, 59, 123520
Lopez R. E., Turner M. S., 1999, Phys. Rev. D, 59, 103502
Lopez R. E., Dodelson S., Heckler A., Turner M. S., 1999, Phys. Rev. Lett., 82, 3952
Mangano G., Miele G., Pastor S., Peloso M., 2002, Phys. Lett. B, 534, 8
Melchiorri A., Griffiths L. M., 2001, New Astron. Rev., 45, Issues 4 and 5
Melchiorri A. et al., 2000, Astrophys. J., 536, L63
Netterfield C. B. et al., 2001, ApJ, accepted (astro-ph/0104460)
Orito M., Kajino T., Mathews G. J., Boyd R. N., 2000, ApJ, submitted (astro-ph/0005446)
Peebles P. J. E., 1993, Principles of Physical Cosmology. Princeton Univ. Press, Princeton, NJ

Percival W. J. et al., 2001, MNRAS, 327, 1297
Perlmutter S. et al., 1997, ApJ, 483, 565
Perlmutter S. et al. (the Supernova Cosmology Project Collaboration), 1999, ApJ, 517, 565
Pryke C., Halverson N. W., Leitch E. M., Kovac J., Carlstrom J. E., Holzapfel W. L., Dragovan M., 2002, ApJ, 568, 46
Saunders W. et al., 2000, MNRAS, 317, 55
Seljak, U., Zaldarriaga M., 1996a, ApJ, 469, 437
Seljak U., Zaldarriaga M., 1996b, Phys. Rev. Lett., 78, 2054
Skordis C., Albrect A., 2002, Phys. Rev. D, submitted (astro-ph/0012195)
Steigman G., 2001, preprint (astro-ph/0108148)
Trotta R., Riazuelo A., Durrer R., 2001, Phys. Rev. Lett., 87, 231301
Turner M. S., 2001, preprint (astro-ph/0106035)
Wang X., Tegmark M., Zaldarriaga M., 2002, Phys. Rev. D, 65, 123001
Weller J., Albrecht A., 2002, Pyhs. Rev. D, 65, 103512
White M., Gelmini G., Silk J., 1995, Phys. Rev. D, 51, 2669
Zaldarriaga M., Spergel D. N., Seljak U., 1997, ApJ., 488, 1
Zentner A. R., Walker T. P., 2002, Phys. Rev. D, 65, 063506

This paper has been typeset from a TEX/LATEX file prepared by the author.